UNIVERSITÀ DEGLI STUDI DI TORINO

Coppola D., Cigolini C. (2013) Thermal regimes and effusive trends at Nyamuragira volcano (DRC) from MODIS infrared data, BULLETIN OF VOLCANOLOGY (ISSN:0258-8900), Vol. 75, pp. 1- 15. http://dx.doi.org/10.1007/s00445-013-0744-z

Thermal regimes and effusive trends at Nyamuragira volcano (DRC) from MODIS infrared data

D. Coppola[1], C. Cigolini[1,2]

1) Dipartimento di Scienze della Terra, Universita` degli Studi di Torino, Via Valperga Caluso 35, 10125 Torino, Italy

2) NatRisk, Centro Interdipartimentale sui Rischi Naturali in Ambiente Montano e Collinare, Universita` degli Studi di Torino, Italy

Email: diego.coppola@unito.it

Keywords: Nyamuragira, Volcanic Radiative Power, thermal regimes, effusive trends, MODIS

Abstract

Nyamuragira volcano is one of the most active African volcanoes. Eruptions have been occurring every 3-4 years throughout the last century. Here, we analyse satellite infrared data, collected by MODIS sensor to estimate the Volcanic Radiative Power (*VRP*, in W) and Energy (*VRE*; in J) released during the 2001, 2002, 2004, 2006-07, 2010 and 2011-12 eruptions. Based on the statistical distribution of *VRP* measurements, we found that thermal emissions at Nyamuragira fall into three distinct radiating regimes. The *High-Radiating Regime* occurs during the emplacement of poorly-insulated lava flows and characterise most of the *effusive activity*. The *Moderate-Radiating Regime* is associated with *open-vent activity* (Strombolian explosions and/or lava lake activity) eventually accompanied by the emplacement of short-lived and well-insulated flows. A third radiating regime (*Low-Radiating Regime*) occurs during periods, which may last weeks to months, that follow each eruption and are associated with the cooling of the effused lava flows.

By applying the radiant density approach to MODIS-derived *VRP* we also estimated the time-averaged lava discharge rates (*TADR*; in m^3 s^{-1}) and we analysed the effusive trends of the above eruptions. We found that the transition between the *effusive* and *open-vent* activity typically takes place when *TADR* reduces to low values (< 5 m^3 s^{-1}) and marks a change in the eruptive style of the volcano. Finally we observed a clear correlation between the volume of erupted lava and its cooling time. This suggests that the average thickness of the analysed lava flows is more variable than previously thought and sheds light on the uncertainty in calculating erupted volumes assuming that lava flow areas have uniform thickness.

1. Introduction

The MODIS instrument (Moderate Resolution Imaging Spectroradiometer), aboard the Terra (EOS AM) and Aqua (EOS PM) satellites, offers a temporal coverage (~4 images day^{-1}), spatial resolution (1 km in the IR bands) and an adequate spectral coverage (the "fire channel" at ~4μm on MODIS band 21) to enable the detection and quantification of thermal emissions related to several types of volcanic activity (Wright et al. 2002; 2004; 2008a; Rothery et al. 2005; Coppola et al. 2013).

MODIS infrared data give the possibility to estimate the radiative power and energy related to the effusive eruptions (Wright and Pilger 2008) and to convert these into first-order eruptive parameters such as time averaged lava discharge rates (*TADR*; in m^3 s^{-1}) and erupted volumes (Harris and Baloga 2009; Harris et al. 2011; Coppola et al. 2013). Although MODIS has been used to quantify volumetric fluxes at basaltic volcanoes, such as Etna (e.g. Steffke et al. 2011; Harris et al. 2011), Stromboli (e.g. Ripepe et al. 2005; Calvari et al. 2010; Coppola et al. 2012), Piton de la Fournaise (Coppola et al. 2009; 2010; Gouhier and Coppola 2011) and Kilauea (Di Bartola et al. 2008, Koeppen et al., 2013), its application in the analysis of Nyamuragira eruptions has addressed only a few, with only qualitative observations (e.g., Wright and Pilger 2008; Wadge and Burt 2011). Nonetheless, Nyamuragira volcano is one of the most active volcanoes in Africa, counting thirty-

eight eruptions since the beginning of the 20th century. Notably, since 1980 the long-term magma output rate at Nyamuragira has increased significantly (from 0.47 m^3 s^{-1} to 1.13 m^3 s^{-1}) and eruptions have been considered to follow the so-called "pressure-cooker" model (Wadge 1981) whereby the eruptions take place when the magma exerts an overpressure that exceeds the wall rocks' strength and the confining pressure (Burt et al. 1994; Wadge and Burt 2011). Thus far, the volumetric fluxes and effusive trends have been only inferred qualitatively (Wadge and Burt 2011) due to limited and sporadic measurements of lava discharge rates within recent years (Smithsonian Institution, 2001 to present).

In addition, a significant fraction of the global volcanic sulphur budget has been ascribed to Nyamuragira volcano (Halmer et al. 2002; Bluth and Carn 2008; Head et al. 2011). Gas release seems to be concentrated within the first 1-3 days of activity (Bluth and Carn 2008) with total SO_2 emissions (measured by satellites) exceeding those produced by syn-eruptive degassing (Head et al. 2011). As outlined by Carn and Bluth (2003) the link between sulphur emissions and erupted lava is an important tool for hazard assessment and *"it would be interesting to determine information regarding the lava/tephra production"* of Nyamuragira eruptions. However, volumetric estimates are currently retrieved from the area of the lava fields and an assumed average thickness (Kasahara 1983; Smets et al. 2010, Head et al 2012). Therefore, there is a need for improved measurements of eruption rates at Nyamuragira.

Here we analyse the long term data recorded by MODIS to differentiate distinct thermal regimes associated to the recent eruptive activity of Nyamuragira (2001 to 2012). Then, we apply the "*radiant density*" approach (Coppola et al. 2013) to estimate Time Averaged lava Discharge Rates (*TADR*) and volumes (*Vol*) for five eruptions (2001, 2002, 2004, 2010, 2011-12). Finally, we describe the observed effusive trends and we relate the calculated volumes to the duration of the cooling process. The assumption of a uniform flow thickness for calculating Nyamiragira lava flow volumes from final area is thus questioned and discussed also in the light of published SO_2 fluxes for the 2001, 2002 and 2004 eruption (Bluth and Carn 2008) .

Figure 1

2 Geological setting and eruptive styles

Nyamuragira volcano (3058 m asl) is located in the Virunga Volcanic Zone (VVZ), a sector of the western branch of the East African Rift, just north of Lake Kivu (Fig. 1). Currently, Nyamuragira and the nearby Nyiragongo volcano, are the only active volcanoes within the western branch.

Nyamuragira lavas are alkali basalts, hawaiites, basanites and tephrites with SiO_2 ranging from 43 to 56 wt% (Aoki et al. 1985). Recently erupted products show a rather restricted compositional range with silica contents from 45.2 to 46.3 SiO_2 wt% (Chakrabarti et al. 2009; Head et al. 2011). Since the 1940s, volcanic activity has been characterized by episodic flank effusive eruptions with intervals of summit lava lake activity (Hamaguchi and Zana 1983). Eruptions are fed by dykes and fissures that occasionally cut the summit caldera (~2 km in diameter), and more often propagate down the flanks of the volcano (Wadge and Burt 2011). Eruption onsets are characterised by the ejection of lava fountains that may reach 200-300 m in height, and may involve one or more fissure vents. In general, fountaining feeds large and fast-moving lava flows that reach lengths of 15-20 km in few days (Smithsonian Institution 2001 to present). The very low amplitude of the pre-eruptive inflation suggests that the vigorous lava fountaining and gas release, typical of this initial activity, is essentially driven by magma decompression rather than by the release of elastic energy stored in the reservoir's wallrocks (Toombs and Wadge, 2012).

Recent satellite-based studies on SO_2 emissions have suggested that the effusive activity is characterized by a strong "excess" of sulfur (Carn and Bluth 2003; Bluth and Carn 2008; Head et al. 2011) clearly exceeding those derived from petrologic models (Wallace 2001; Sharma et al., 2004, Shinohara 2008). Between 1980 and 2004 (14 eruptions) the total SO_2 output was estimated to be nearly 25 Mt (Bluth and Carn 2008), whereas to the total dense rock equivalent (DRE) volume of

lava erupted during the same period reached approximately 1 km^3 (Wadge and Burt 2011). In order to reconcile the measured SO_2 emissions of Nyamuragira with the amount of erupted lava, an initial S content of about 5000 ppm in the Nyamuragira magma is required, although the maximum S content found in the primitive melts is nearly 3700 ppm (Head et al. 2011). This imbalance led Head et al. (2011) to suggest that an additional source for SO_2 may be explained by the following: (1) accumulation of a vapor phase within the magmatic system that is solely released during eruptions; (2) syn-eruptive gas release from unerupted magma.

Following the intense lava and gas production occurring during the early stages of eruption, lava effusion often diminishes gradually before ceasing (Bluth and Carn 2008; Wadge and Burt 2011; Head et al. 2012). A transition from Hawaiian-type fountaining to Strombolian activity may eventually occur (Ueki 1983; Burt et al. 1994). Due to the lack of field observations, the date of the end of the eruption is often uncertain (Wadge and Burt 2011).

3. MODIS analysis of recent Nyamuragira eruptions (2001-2012)

3.1 - Volcanic Radiative Power (VRP) and Energies (VRE) at Nyamuragira

MODIS data have been used to estimate the Volcanic Radiative Power (*VRP* in W) and Volcanic Radiative Energy (*VRE* in J) produced by the Nyamuragira eruptions between 2001 and 2012 (e.g., 2001, 2002, 2004, 2006-7, 2010, 2011-12). A description of the method used to calculate *VRP* and *VRE* from MODIS data is given in Coppola et al. (2013). Here, in addition to the data processing described by Coppola et al. (2013), we apply a correction for those images affected by pixel saturation on MODIS channel 21 (centred at 3.959 μm). A detailed description of this procedure is given in the supplementary material.

In order to exclude the thermal anomalies caused by the activity of the neighbour Nyiragongo volcano, which hosts a very active lava lake at its summit, we applied a predefined spatial mask that allowed us to eliminate all the hot-spot contaminated pixels located within an area of 5 x 5 km around the summit of Nyiragongo.

Importantly, we checked by eye all the MODIS images to validate the location of thermal anomalies (when detected) and to classify the data as "*unsuitable"*, when the thermal emission was clearly attenuated by the presence of clouds or by the volcanic plume. Note that during this final step we manually discarded all the images where the thermal signal was "undoubtedly" affected or completely masked by the above. However, we cannot exclude that over the entire dataset some of the images considered as *suitable* may still be affected by a moderate degree of attenuation. On the whole, over a total of 826 alert-bearing MODIS overpasses, we classified as *suitable* only 318 images (~38.5% of the total detections).

Figure 2

The complete *VRP* time-series recorded at Nyamuragira between 2001 and 2012 is shown in Fig. 1h (black stem), whereas in Figs 1b to 1g we report the MODIS-derived thermal anomaly maps for each eruption (overprinted over a shaded relief map of the area). These have been obtained by plotting, for each alerted pixel, the highest value of radiance (within a normalised color-scale), recorded during each eruption.

The detailed time-series of each eruption (including the *unsuitable* data) are reported in Fig. 2a to 2f.

Here we plotted the *VRP* (including the *unsuitable* data) on logarithmic scale and we classify the data according to the different thermal regimes described in the next chapter. We also plotted the Volcanic Radiative Energy (*VRE*) representing the cumulative thermal energy radiated by the eruption. This last has been calculated as the trapezoidal integration of the *VRP* time-series,

assuming a linear trend between two consecutive *suitable VRP* measurements (blue lines in Fig. 2). The estimated error of the total energy radiated by each single eruption is ± 30%.

The Volcanic Radiative Energies (*VRE*) of each eruption are summarised in Table 1 where we also reported the relative final lava flow area from published data (Smet et al. 2010). Note that there were not sufficient *suitable* images for calculating the *VRE* of the 2006 eruption, thus this event has been excluded from our analysis.

Table 1

3.2 – Thermal regimes at Nyamuragira volcano

The dataset of *suitable* images (318 data) indicates that the *VRP* detected at Nyamuragira ranges from ~2 to ~79594 MW (with a mean μ_{VRP} = 4599 MW and standard deviation σ_{VRP} = 8150 MW), thus spanning over four orders of magnitude.

As observed in several *VRP* time-series of other volcanoes, the frequency distributions of Volcanic Radiative Power are extremely peaked and strongly asymmetric toward the higher values (e.g. Coppola et al. 2012). To better visualise the shape and properties of such asymmetric distributions, we transformed the original data (*VRP*) into log-data (*log[VRP]*), a procedure that was used to identify distinct thermal regimes at Stromboli volcano (Coppola et al. 2012).

At Nyamuragira, the frequency histogram of the recorded *log[VRP]* (binned into 25 classes in Fig. 3a) reveals the presence of a composite distribution, with at least two main groups that characterise distinct thermal regimes (Fig. 3a). Such a bimodal distribution is also evident within the normal probability plot for *log[VRP]* (Fig. 3b). Here, the log-transformed data define two distinct trends that intersect at about 2000 MW. Notably, these two regimes are almost equally represented within the *suitable* dataset, each one occurring with a probability of ~50% (Fig. 3b).

Figure 3

Deeper insights into Nyamuragira's thermal regimes were obtained by considering the radiative power emitted exclusively by the "most radiant" pixel detected within each *suitable* image, hereby defined VRP_{MAX}. Unlike the *VRP*, which measures the heat radiated by the whole active lava flow, the VRP_{MAX} represents a measurement of how much the hottest lava is spatially concentrated within the most active portion of the lava flow.

The frequency distribution of $log[VRP_{MAX}]$, and related normal probability plots shows that this parameter has a rather complex distribution and can be subdivided into four groups (Fig. 3c and 3d). However, the group with the highest VRP_{MAX} (>1300 MW) includes the data where the correction of saturated pixel was applied (see supplementary material). Due to the resampling process, the *VRPmax* of the images affected by pixel saturation is somehow corrupted by the adjacent pixels. Therefore we believe that this statistical group is not a real thermal regime but is essentially an analytic artefact and should not be taken into account (Fig. 3d). Conversely, the distribution of the rest of the data define three groups that reflect three distinct radiating regimes. Based on the statistical distributions of both *VRP* and VRP_{max} we thus suggest that the thermal emissions at Nyamuragira may be subdivided into the following regimes: *High-Radiating Regime* (*HRR*), *Moderate-Ratiating Regime* (*MRR*) and *Low-Radiating Regime* (*LRR*).

The *High-Radiating Regime* (*HRR*) is represented by thermal anomalies characterised by *VRP* > 2000 MW (142 data) and represents ~45% of the whole dataset (Fig. 3a and 3b). This regime is typically, but not always, associated to a VRP_{MAX} higher than 200 MW (Fig. 3c and 3d). Highest thermal emissions (*VRP* = 20000-70000 MW, or 95 percentile) are generally recorded during the first week of activity which follows the onset of single eruptions (Fig. 2). This is due to the occurrence of high lava fountains (hundred of meters high) and/or extended channel-fed lava flows

commonly observed in the field (Smithsonian Institution, 2001 to present). The *HRR* is always associated with large thermal anomalies that may extend up to 15-20 km from the active vent(s) (Fig. 4a) and normally persist without interruption up to the transition into the *MRR*. Notably, for the 2001, 2002, 2004 and 2010 eruptions the duration of *HRR* was extremely regular (24-26 days) but during the last eruption (2011-2012) it was much longer, reaching 110 days (Table 1).

Moderate-Radiating Regime (MRR) is characterised by all the data having VRP< 2000 MW and VRP_{MAX} > 10 MW (59 data). The *MRR* represents about 18% of the whole dataset (Fig. 3d). This regime was essentially recorded during the late stages of each eruption and follows an evident decrease of *VRP* (Fig. 2). During the analysed eruptions the *MRR* lasted from 4 to 38 days (Table 1), followed by a transition to the *LRR*. Usually, the *Moderate-Radiating Regime* is characterised by decreasing thermal emissions accompanied by focussing on the anomaly around the vent area (Fig. 4b). A transition from Hawaiian-type (fountain-fed) *effusive activity* to Strombolian-type, *open vent activity*, has been frequently observed in the late stages of Nyamuragira eruptions (e.g. Smithsonian Institution 2000 to present, Head et al. 2011) and may explain both the reduction of the thermal power as well as the focussing of the anomaly above the vent area. Thus, we associate the *MRR* with the terminal stage of the Nyamuragira's eruptions, when the moderate thermal emissions are essentially produced by an *open vent activity:* either Strombolian or lava lake activity, or both. Eventually, this regime may be accompanied by the emplacement of well-insulated and short-lived lava flows emplaced nearby the vent (i.e., pahoehoe sheet flows).

Figure 4

The third group is represented by thermal anomalies with VRP_{MAX} < 10 MW (117 data; ~37%) that belong to the *Low-Radiating Regime* (*LRR*). This regime occurs as a gradual evolution of *MRR* and represents the very last period of thermal anomalies detected during each eruption. These are

generally located above the vent area and/or above the central portion of the lava flow field without showing any particular spatial clustering (Figure 4c). The duration of *LRR* varied from 21 to 212 days (Table 1) and according to the reports of Smithsonian Institution (2001 to present) no effusive activity has been ever reported during this regime. We thus regard the *LRR* as associated to the cooling of the lava flow fields that were previously emplaced. The presence of fractures and cracks (still hot), may effectively produce a residual thermal anomalies (within the thickest portion of the flow fields) that may persist for several weeks or months.

4 – Time Averaged lava Discharge Rates (TADR) from MODIS-derived VRP: the radiant density approach

When derived from satellite thermal data, lava discharge rates are generally obtained using the heat budget model developed by Pieri and Baloga (1986) and later refined by Crisp and Baloga (1990) and Harris et al. (1997; 1998). Further, Wright et al. (2001) found that rather than being used to calculate heat loss, the original Pieri and Baloga's approach uses the satellite data to estimate the area of active lava flows at the moment of a satellite overpass. Accordingly, the thermal approach relies simply on an empirical relationship *whereby, under given insulation, rheological and ambient conditions, the active flow area is proportional to "Time Averaged lava Discharge Rate (TADR)* (Harris and Baloga, 2009):

$$TADR = A_{active}\, x \qquad (1)$$

where x is the coefficient of proportionality which needs to be settled for any specific thermal, rheological, compositional and ambient (e.g., slope and flow bed roughness) conditions (Harris and Baloga, 2009; Harris et al., 2010). Based on this alternative approach Coppola et al. (2013) recently proposed an empirical method to relate the Time Averaged lava Discharge Rates (*TADR*) to the Volcanic Radiative Power (*VRP*) estimated via MODIS. This method is based on a unique best-fit coefficient, defined as "*radiant density*" (c_{rad}), that integrates all the appropriate insulation, rheological and topographic conditions given by the proportionality between lava discharge rate and

active area (embedded within *x*). In particular, the radiant density approach assumes that during a *suitable* MODIS acquisition, the *VRP* is related to the heat produced exclusively by the "active" flow area (A_{active}) with radiating temperature (*Te*) equal or higher than 600 K so that:

$$VRP = A_{active}\sigma\varepsilon T_e^4 \quad (2)$$

where σ and ε are the Stephan Boltzmann constant and the emissivity, respectively. Accordingly, the *TADR* ($m^3\ s^{-1}$) is related to the *VRP* (W) through the following relationship:

$$TADR = A_{active}x = A_{active} \times \frac{\sigma\varepsilon T_e^4}{c_{rad}} = \frac{VRP}{c_{rad}} \quad (3)$$

being c_{rad} ($J\ m^{-3}$) the radiant density of the "active" lava flow:

$$c_{rad} = \frac{\sigma\varepsilon T_e^4}{x} \quad (4)$$

with the same notations in equations (1) and (2).

Based on a solid dataset that includes basaltic lava flow and silicic domes, Coppola et al. (2013) introduced an empirical relationship that relates the radiant density to the silica content of the erupted lavas. This relationship is expressed as:

$$c_{rad} = 6.45 \times 10^{25} \times \left(X_{SiO_2}\right)^{-10.4} \quad (5)$$

where X_{SiO2} is the silica content (wt%) of the erupted lava.

For Nyamuragira we settled X_{SiO2} = 45.7 wt% (i.e., the average silica content of recently erupted products; Chakrabarti et al. 2009; Head et al. 2011) in equation (5), and we obtain a c_{rad} equal to 3.5 × 10^8 J m^{-3}. This value represents an average estimate and, according to Coppola et al. (2013), has an uncertainty of ± 50% due to the errors in calculation of radiative energies and independent volumes. Nonetheless, this uncertainty embeds all the combinations of *Te* and *x* able to describe the proportionality between *TADR* and active flow area (Coppola et al., 2013). Hence, for Nyamuragira, we settled a c_{rad} between 1.75 × 10^8 and 5.25 × 10^8 J m-^{3}, that likely incorporate all the possible combinations of insulation, rheological and topographic conditions operating during the emplacement of the lava flows. From any suitable *VRP* measurement we thus estimated the *TADR*

(± 50%) by using equation (3) and the two end-member radiant densities cited above (1.75 to 5.25 × 10^8 J m^{-3}).

5 - Effusive trends

Lava discharge rates were calculated according to the above procedure and the resulting time-series are reported in Fig. 5 to 9. A detailed description of the effusive trends is presented in the next sections where all times are given in UTC (Universal Time Coordinated).

Figure 5

5.1 - 2001 eruption

The 2001 eruption started on February 5 at 20:45 (Smithsonian Institution 2001). On February 7, two lava flows, ~10 km in length, were detected by MODIS on the northern and southern flanks of the volcano (Fig. 5). By that time the northern flow was more active and reached a *TADR* of 172 (± 86) m^3 s^{-1}. The southern flow showed a *TADR* of 15 (± 7.5) m^3 s^{-1}. In the following days, the effusive trend of the northern branch strongly decreased until February 12, when a new pulse reactivated the eruption with *TADR* of ~80 (± 40) m^3 s^{-1} (which affected both the eruptive fissures). In the next days, lava effusion onto the northern flank showed an exponential decay and ceased on March 1. By mid-February the southern flow became the most active with *TADR* of 60 (± 30) m^3 s^{-1} and then decreased to 20 (± 10) m^3 s^{-1} at the end of the month. A short pulse in lava effusion from the southern fissure (with *TADR* = 50 ± 25 m^3 s^{-1}), was detected on March 2nd and was coeval with the end of activity onto the northern flank (Fig. 5). A few days later, the activity at southern flank vent decreased and thermal emissions switched to the *Moderated-Radiating Regime* (with *TADR* declining from 5 ± 2.5 to less than 2 ± 1 m^3 s^{-1}). Activity on the southern flank ceased definitely by March 11, 2001. In the following days volcanologists reported that three cones had formed on the

southern eruptive fracture and one of them was still hot during their survey (Smithsonian Institution 2001).

5.2 - 2002 eruption

On July 25, 2002 (at 11:10) a new eruption started, involving two km-long fractures that affected the northern and southern flanks of Nyamuragira and part of the summit caldera (Toombs and Wadge 2012). A few hours later a MODIS image revealed the presence of two large lava flows on northern and southern flanks (~7.5 km-long and ~5 km-long, respectively), together with a clear evidence of effusive activity within the summit caldera (Fig. 6). By that time the total *TADR* was 109.2 (± 54.6) m^3 s^{-1} and was almost equally subdivided between the northern, summit and southern activity. On July 27 at 23:30, the effusive activity at the summit and along the southern flank completely ceased. The lava flow on the northern side was still active and the *TADR* peaked at 303.2 (± 151.6) m^3 s^{-1}. By this time the front of the northern flow had further reached ~12 km in length (Fig. 6). In the next days the eruption continued onto the northern flank. We detected a decay of *TADR* coupled with a progressive migration of the surface anomalies toward the vent area with MODIS-derived *TADR* measuring 38.6 (±19.3) m^3 s^{-1} on August 5, 2002. Notably, this is in excellent agreement with field observations on August 6, 2002 that estimated a lava discharge rate of ~35 m^3 s^{-1} (Smithsonian Institution 2002; black star in Fig.6).

By August 20, 2002, the *TADR* had further declined to 7.9 (± 3.9) m^3 s^{-1}, and thermal emissions shifted to the *Moderate-Radiating Regime* (MRR). The *MRR* of the 2002 eruption lasted 38 days with a permanent hot-spot visible above the vent area (Fig. 6). The *MRR* was characterised by *TADR* ranging from 1.7 (±0.9) to 0.2 (±0.1) m^3 s^{-1} and, according to our data, finally ceased on September 27, 2002.

Figure 6

5.3 –2004 eruption

A new eruption at Nyamuragira volcano started on May 8, 2004. In contrast to the previous eruptions, in this case we did not record a clear waning trend but we were able to detect effusive pulses (up to 120 ± 60 m^3 s^{-1}) that were overprinted on an almost stable discharge rate (around 30-50 m^3 s^{-1}) lasting 24 days (Fig. 7). We think that initially higher lava discharge rates could not be detected due to the presence of thick ash plumes (produced on the first days of activity; Smithsonian Institution 2004). However, the unusual behaviour of the 2004 eruption was also noticed by the Goma Volcano Observatory (GVO) staff who reported that "*the activity remained quite strong and apparently stable in comparison with other documented Nyamuragira eruptions*" (Smithsonian Institution 2004).

Our estimates suggest that at least three pulses characterised this eruption, each one coeval with the emplacement of a new sector of the lava field. This last made an intricate delta below the lower cone, turning into a lava flow that reached a length of ~12 km (Smithsonian Institution 2004).

Our data suggest that the initial effusive activity affected the summit caldera and later propagated onto the northern flank with the emplacement of a 10 km long lava flow (*TADR* were in the order of ~90 ±45 m^3 s^{-1}). On May 13 the effusive activity decreased to 50 (± 25) m^3 s^{-1} and later, on May 15, a new effusive pulse (up to 125.8 ± 62.9 m^3 s^{-1}) produced lava advancement toward the NW (Fig. 7). By this time the lava flow reached 12 km in length. Following this pulse the effusive activity gradually decreased and lava emplacement was concentrated within the central part of the flow field (Fig. 7).

On May 27 a second pulse was detected by MODIS that was associated to a renewed effusive activity (up to 124.3 ± 62.2 m^3 s^{-1}) within the central sector of the flow field (Fig. 7). Interestingly, this increase was accompanied by the resurgence of a low-amplitude thermal anomaly within the caldera, likely associated with a short-lived effusive activity at the summit vent. The final pulse occurred on 31 May 2004 (*TADR* = 65.6 ± 32.8 m^3 s^{-1}), and was associated to lava emplacement

onto the easternmost sector of the lava field (Fig. 7). Since June 1 the activity shifted toward the *MRR* and persisted until 14 June 2004.

Figure 7

5.4 - 2010 eruption

The 2010 eruption lacks any evidence of a waning effusive trend (Fig. 8). High amounts of SO_2 and ash were released during the first week of the eruption (Smithsonian Institution 2010) and likely may have prevented the detection of large thermal anomalies during the initial stages of this eruption. Similarly to the 2004 eruption, the moderately fluctuating trend of the effusive pattern suggests relatively mild effusion rates (15-30 $m^3 s^{-1}$) interrupted by short periods of higher (~ 64 ± 32 $m^3 s^{-1}$) and lower (~6.5 ± 3.2 $m^3 s^{-1}$) *TADRs*. Thermal emissions shifted into the *MRR* on January 27, 2010 and persisted a couple of days only before the end of the eruption. The summit caldera was involved in the effusive activity only during the first week of the eruption.

Figure 8

5.5 – 2011-12 eruption

The 2011-12 eruption started on November 6, 2011 at 03:55, following two days of intense seismicity (Smithsonian Institution 2011). Lava effusion occurred from a fissure located at about 12 km ENE of the main crater with an orientation of ~N70°E.

The effusive trend of the 2011-12 eruption (Fig. 9) was characterised by a long lasting effusive phase (*High-Radiating Regime – HRR,* lasting 110 days) followed by a terminal phase of *Moderate-Radiating Regime (MRR)* lasting 33 days (Table 1). This final stage of *open-vent* activity was

coeval with the gradual surfacing of a small thermal anomaly within the summit caldera of Nyamuragira (Coppola, unpublished data) likely associated to shallow degassing event observed within the pit crater since April 2012 (Virunga National Park 2012). We estimated that 252 (±126) Mm^3 of lava were emplaced during the 2011-2012 flank eruption that make this event one of the most voluminous eruptions occurred at Nyamuragira volcano in the last century (Wadge and Burt 2011). Based on a Landsat ETM+ (Enhanced Thematic Mapper Plus) image collected on March 28, 2012, we estimated that the final lava field had covered an area of ~26.8 km^2 with a maximum length of ~11.3 km.

Figure 9

A particular feature recorded during all the above eruptions is the transition from the *effusive* to the *open vent activity* (from *HRR* to *MRR*). This transition precedes the ceasing of an eruption and is independent from the duration of the following *MRR* (which may last from few days to several weeks). According to our estimates this transition occurs at lava discharge rates of ~5 m^3 s^{-1} and is a prelude to a change in the eruptive style of the volcano.

6 - MODIS-derived volumes and lava flows thicknesses

The trapezoidal integration of the *TADR* time-series allowed us to estimate the cumulative volumes of erupted lava for each single eruption (Table 1). As previously discussed, we assumed the end of the *MRR* as the end of the eruptive event considered. In Figure 10a we compared the MODIS-derived volumes with the final lava flow plan areas measured by Smets et al. (2010) (for the 2011 eruption we used our estimate). In this framework, our best volume estimates for the 2001, 2002, 2004 and 2010 lava flows are consistent with lava flow thicknesses of 3 to 6 m (grey field in Fig.

1a), even though the uncertainty of these measures encompass a range of thicknesses between 1.5 and 8 m.

For the 2011-12 eruption we calculated a volume of 252 (± 126) Mm^3 that, given a flow area of ~26.8 km^2 estimates the average flow thickness as 9.4 (±4.7) m. Since the silica contents of lava flows did not substantially change during recent eruptions (cf., Chakrabarti et al., 2009; Head et al., 2011), we believe that this greater thickness is essentially related to the emplacement mechanism of this lava field, likely characterised by the overlapping of several flow units. This occurred over a period that lasted 4-5 times longer than the previous eruptions, although it emplaced a lava flow field with comparable areal extent (see Table 1). The correlation between the MODIS-derived volumes and the duration of the *Low-Radiating Regime* (ascribed to the cooling of the lava flow fields)(Fig. 10b) indicates that the 2011-12 lava volume took much longer to cool down, which is consistent with a greater thickness of this lava field with respect to the previous ones. The linear correlation shown in Fig 10b thus outlines the causal link between lava flow volumes and the duration of cooling processes. This supports the idea that the average thickness of the analysed lava flows was not uniform, but varied by several meters thus causing the different cooling times. Hence, we suggest that the assumption of a fixed flow thickness (i.e. 3 m at Nyamuragira; Smets et al., 2010 and reference therein) may lead to significant errors in the estimate of erupted volumes from lava flow areas. This will be inevitably reflected in errors of the magma output rates as well as in the quantification of the sulfur excess characterizing Nyamuragira eruptions (Head et al., 2011).

For example by assuming a bulk magma density ρ_m=2340 kg m^{-3} (equal to DRE ρ_m= 2600 with an assumed vescicularity of 10%), a crystal mass fraction of 0.1 (Aoki et al, 1985) and an initial sulfur content ranging from 1800 to 3700 ppm (cf., the maximum sulfur contents in melts; Head et al., 2011), we may apply the petrological method (Wallace, 2001, Sharma et al., 2004) to tentatively convert our best volume estimates (Table 1) into the mass of "syn-eruptive" SO_2. We thus estimate 1.61±0.55 Mt, 1.22±0.42 Mt and 1.28±0.44 Mt of SO_2 for the 2001, 2002 and 2004 eruptions respectively. These values are compared with those measured during the same eruptions by the

OMI instrument (Bluth and Carn, 2008): being 1.73 Mt, 2.32 Mt and 2.6 Mt of SO_2, respectively. While for the 2001 eruption the two estimates are in some ways consistent, for the 2002 and 2004 eruptions the comparison indicates an excess of sulphur degassing, which could be explained by a portion of "unerupted" magma amounting approximately to ~0.1 km^3. Note that by applying the petrological method to the volumes estimated by Smets et al., (2010) for the 2002 and 2004 eruptions (which assumed a uniform thickness of 3 m) we obtain only 0.66±0.23 Mt and 0.79±0.44 Mt of SO_2, respectively, a range of values which would increase the apparent SO_2 excess. Although this comparison is preliminary and subject to large uncertainties, our results reveal that the excess of SO_2 does not seem to characterize all Nyamuragira eruptions. An exhaustive discussion concerning the comparison between magma and SO_2 fluxes is beyond the scope of this paper. However, we trust that our data can be used to better analyze the gas-magma partitioning at Nyamuragira volcano (Head et al., 2011) shading light on the origin of its sulfur excess.

Figure 10

Conclusions

In this paper we showed the potential of using satellite-based infrared data for observing volcanic activity at Nyamuragira. In particular, the measurements of Volcanic Radiative Power (*VRP*) and Energy (*VRE*) produced by each eruption and their long term trends gave us the opportunity to identify three different radiating regimes. The first two regimes (*HRR* and *MRR*) are related to the *effusive* and *open vent* activity, whereas the third regime (*LRR*) is due to the cooling process that follows the emplacement of lava fields. We suggest that in the absence of direct observation, this classification can be used to monitor changes in the eruptive style and/or to detect the ceasing of an effusive eruption. Finally we show that the radiant density approach can be used for estimating the lava discharge rates and erupted volumes during future eruptions of Nyamuragira. We thus suggest

that the integration of MODIS-derived effusive trends with additional geochemical - geophysical datasets (i.e. SO_2 flux, deformation) will certainly contribute to better assess the eruption dynamics of this very active volcano.

Acknowledgements

We acknowledge Sonia Calvari, Geoff Wadge and an anonymous reviewer for providing useful comments and suggestions that greatly improved our earlier manuscript. We also acknowledge the NASA-LAADS (http://ladsweb.nascom.nasa.gov/) for providing level 1b MODIS data. Digital Elevation Model are courtesy of CGIAR (srtm.csi.cgiar.org). This research was supported by the Italian Ministry for Universities and Research (MIUR).

References

Aoki K, Yoshida T, Yusa K, Nakamura Y, (1985) Petrology and Geochemistry of the Nyamuragira Volcano, Zaire. J Volcanol Geotherm Res 25: 1-28.

Bluth GJS, Carn SA (2008) Exceptional sulphur degassing from Nyamuragira volcano, 1979–2005. Int J Remote Sens 29(22): 6667–6685. doi:10.1080/ 01431160802168434.

Burt ML, Wadge G, Scott WA (1994) Simple Stochastic modelling of the eruption history of a basaltic volcano: Nyamuragira, Zaire. Bull Volcanol 56(2): 87–97.

Calvari S, Lodato L, Steffke A, Cristaldi A, Harris AJL, Spampinato L, Boschi E (2010) The 2007 Stromboli flank eruption: chronology of the events, and effusion rate measurements from thermal images and satellite data. J Geophys Res 115 (B4), B04201. doi:10.1029/2009JB006478.

Carn SA, Bluth GJS (2003) Prodigious sulfur dioxide emissions from Nyamuragira volcano, D.R. Congo. Geophys Res Lett 30(23), 2211. doi:10.1029/2003GL018465.

Chakrabarti R, Basu AR, Santo AP, Tedesco D, Vaselli O (2009) Isotopic and geochemical evidence for a heterogeneous mantle plume origin of the Virunga volcanics, Western rift, East African Rift system. Chem Geol 259: 273-289. doi:10.1016/j.chemgeo.2008.11.010.

Coppola D, Piscopo D, Staudacher T, Cigolini C (2009) Lava discharge rate and effusive pattern at Piton de la Fournaise from MODIS data. J Volcanol Geotherm Res 184 (1–2): 174–192.

Coppola D, James MR, Staudacher T, Cigolini C (2010) A comparison of field- and satellite-derived thermal flux at Piton de la Fournaise: Implications for the calculation of lava discharge rate. Bull Volcanol 72 (3): 341–356.

Coppola D, Piscopo D, Laiolo M, Cigolini C, Delle Donne D, Ripepe M (2012). Radiative heat power at Stromboli volcano during 2000–2011: twelve years of MODIS observations. J Volcanol Geotherm Res 215–216: 48–60.

Coppola D, Laiolo M, Piscopo D, Cigolini C (2013) Rheological control on the radiant density of active lava flows and domes. J Volcanol Geotherm Res 249: 39–48. doi: 10.1016/j.jvolgeores.2012.09.005

Crisp J, Baloga S (1990) A method for estimating eruption rates of planetary lava flows. Icarus 85: 512–515.

Devine JD, H Sigurdsson, A, Davis N, Self S (1984) Estimates of sulfur and chlorine yield to the atmosphere from volcanic eruptions and potential climatic effects, J Geophys Res 89: 6309–6325.

Di Bartola C, Hirn B, Ferrucci F (2008) Spaceborne monitoring 2000-2005 of the Pu'u O'o-Kumaianaha (Hawaii) eruption by synergetic merge of multispectral payloads ASTER and MODIS. IEEE T. Geoscience and Remote Sensing 48(10): 2848-2856

Gouhier M, Coppola D (2011) Satellite-based evidence for a large hydrothermal system at Piton de la Fournaise volcano (Reunion Island). Geophys Res Lett 38 (L02302). doi:10.1029/2010GL046183

Halmer MM, Schmincke HU, Graf HF (2002) The annual volcanic gas input into the atmosphere, in particular into the stratosphere: A global data set for the past 100 years. J Volcanol Geotherm Res 115: 511–528. doi:10.1016/ S0377-0273(01)00318-3.

Hamaguchi H, Zana N (1983) Introduction to volcanoes Nyiragongo and Nyamuragira, in Volcanoes Nyiragongo and Nyamuragira: Geophysical Aspects. Edited by H. Hamaguchi, pp. 1–6, Tohoku Univ., Sendai, Japan.

Harris AJL, Blake S, Rothery DA (1997) A chronology of the 1991 to 1993 Mount Etna eruption using advanced very high resolution radiometer data: implications for real-time thermal volcano monitoring. J Geophys Res 102 (B4): 7985–8003.

Harris AJL, Flynn LP, Keszthelyi L, Mounginis-Mark PJ, Rowland SK, Resing JA (1998) Calculation of lava effusion rates from Landsat TM data. Bull Volcanol 60: 52–71.

Harris AJL, Baloga SM (2009) Lava discharge rates from satellite-measured heat flux. Geophys Res Lett 36 (L19302). doi: 10.1029/2009GL039717

Harris AJL, Favalli M, Steffke A, Fornaciai A, Boschi E (2010) A relation between lava discharge rate, thermal insulation, and flow area set using lidar data. Geophys Res Lett 37 (L20308). doi:10.1029/2010GL044683

Harris AJL, Steffke A, Calvari S, Spampinato L (2011) Thirty years of satellite-derived lava discharge rates at Etna: Implications for steady volumetric output. J Geophys Res 116 (B08204). doi:10.1029/2011JB008237

Head EM, Shaw AM, Wallace PJ, Sims KWW, Carn S (2011) Insight into volatile behavior at Nyamuragira volcano (D.R. Congo, Africa) through olivine-hosted melt inclusions. Geochem Geophys Geosyst 12 (Q0AB11). doi:10.1029/2011GC003699.

Head EM, Maclean AL, Carn SA (2012) Mapping lava flows from Nyamuragira volcano (1967–2011) with satellite data and automated classification methods. Geomatics, Natural Hazards and Risk 4 (2): 119-144. doi: 10.1080/19475705.2012.680503

Kasahara M (1983) Near-field Tilt Measurements Related to the 1981-1982 Nyamuragira Eruption. In: Hamaguchi H (Ed.) Volcanoes Nyiragongo and Nyamuragira: Geophysical Aspects. The Faculty of Science, Tohoku University, Sendai, Japan pp. 47-54.

Koeppen, W.C., Patrick, M., Orr, T., Sutton, J., Dow, D., and Wright, R. (2013). Constraints on the partitioning of Kilauea's lavas between surface and tubed flows, estimated from infrared satellite data, sulfur dioxide flux measurements, and field observations. Bull Volcanol 75: 216. doi:10.1007/s00445-013-0716-3

Mavonga T, Kavotha KS, Lukaya N, Etoy O, Durieux J (2006) Seismic activity prior to the May 8, 2004 eruption of volcano Nyamuragira, Western Rift Valley of Africa. J Volcanol Geotherm Res 158: 355–360

Mavonga T, Kavotha KS, Lukaya N, Etoy O, Mifundu W, Bizimungu RK, Durieux J (2010a) Some aspects of seismicity prior to the 27 November 2006 eruption of Nyamuragira volcano and its implication for volcano monitoring and risk mitigation in the Virunga area,Western Rift Valley of Africa. J African Earth Sciences 58: 829–832

Mavonga T, Zana N, Durrheim RJ (2010b) Studies of crustal structure, seismic precursors to volcanic eruptions and earthquake hazard in the eastern provinces of the Democratic Republic of Congo. J African Earth Sciences 58: 623-633

Pieri DC, Baloga SM (1986) Eruption rate, area, and length relationships for some Hawaiian lava flows. J Volcanol Geotherm Res 30: 29–45.

Ripepe M, Marchetti E, Ulivieri G, Harris AJL, Dehn J, Burton MR, Caltabiano T, Salerno GG (2005) Effusive to explosive transition during the 2003 eruption of Stromboli volcano. Geology 33: 341–344.

Rothery DA, Coppola D, Saunders C (2005) Analysis of volcanic activity patterns using MODIS thermal alerts. Bull Volcanol 67: 539–556.

Sharma K., Blake S., Self, S., Krueger A.J., (2004), SO2 emissions from basaltic eruptions, and the excess sulfur issue. Geophys Res Let 31 (L13612). doi:10.1029/2004GL019688

Shinohara H (2008) Excess degassing from volcanoes and its role on eruptive and intrusive activity. Rev Geophys 46 (RG4005). doi:10.1029/2007RG000244

Smets B, Wauthier C, d'Oreye N (2010) A new map of the lava flow field of Nyamulagira from satellite imagery. J. African Earth Sciences 58: 778–786

Smithsonian Institution (2001) Nyamuragira. Bulletin Global Volcanism Network, Smithsonian Institution, 01/2001; 03/2001 (BGVN 26:01; 26:03).

Smithsonian Institution (2002) Nyamuragira. Bulletin Global Volcanism Network, Smithsonian Institution, 07/2002; 10/2002 (BGVN 27:07; 27:10).

Smithsonian Institution (2004) Nyamuragira. Bulletin Global Volcanism Network, Smithsonian Institution, 04/2004 (BGVN 29:04).

Smithsonian Institution (2007) Nyamuragira. Bulletin Global Volcanism Network, Smithsonian Institution, 01/2007 (BGVN 32:01).

Smithsonian Institution (2010) Nyamuragira. Bulletin Global Volcanism Network, Smithsonian Institution, 08/2010 (BGVN 35:08).

Smithsonian Institution (2011) Nyamuragira. Weekly Reports. http://www.volcano.si.edu/world/volcano.cfm?vnum=0203-02=&volpage=weekly#Nov2011

Steffke AM, Harris AJL, Burton M, Caltabiano T, Salerno GG (2011) Coupled use of COSPEC and satellite measurements to define the volumetric balance during effusive eruptions at Etna, Italy. J Volcano Geotherm Res 205: 45–53. doi: http://dx.doi.org/10.1016/j.jvolgeores.2010.06.004.

Toombs A, Wadge G (2012) Co-eruptive and inter-eruptive surface deformation measured by satellite radar interferometry at Nyamuragira volcano, D.R. Congo, 1996 to 2010. J Volcanol Geotherm Res 245–246: 98–122

Ueki S (1983) Recent volcanism of Nyamuragira and Nyiragongo. In: Hamaguchi, H. (Ed.), Volcanoes Nyiragongo and Nyamuragira: geophysical aspects. Faculty of Science, Tohoku University, Sendai, Japan, pp. 7–18.

Virunga National Park (2012) at http://gorillacd.org/2012/04/25/nyamulagira-volcanos-latest-activity/

Wadge G (1981) The variation of magma discharge during basaltic eruptions. J Volcanol Geotherm Res 11: 139–168.

Wadge G, Burt L (2011) Stress field control of eruption dynamics at a rift volcano: Nyamuragira, D.R. Congo. J Volcanol Geotherm Res 207: 1–15.

Wallace PJ (2001) Volcanic SO_2 emissions and the abundance and distribution of exsolved gas in magma bodies. J Volcanol Geotherm Res 108 85-106.

Woods AW, Bokhove O, de Boer A, Hill BE (2006). Compressible magma flow in a two-dimensional elastic-walled dike. Earth Planet Sci Lett 246: 241–250

Wright R, Blake S, Harris AJL, Rothery DA (2001) A simple explanation for the space-based calculation of lava eruption rates. Earth Planet Sci Lett 192:223–233

Wright R, Flynn L, Garbeil H, Harris A, Pilger E (2002) Automated volcanic eruption detection using MODIS. Remote Sensing of Environment 82: 135–155

Wright R, Flynn LP, Garbeil H, Harris AJL, Pilger E (2004) MODVOLC: near-realtime thermal monitoring of global volcanism. J Volcanol Geotherm Res 135: 29–49. http://dx.doi.org/10.1016/j.jvolgeores.2003.12.008

Wright R, Pilger E (2008a) Radiant flux from Earth's sub-aerially erupting volcanoes. Int J Remote Sensing 29(22): 6443 – 6466. doi: 10.1080/01431160802168210

Zana N, Tanaka K, Kasahara M (1992) Main geophysical features related to the Virunga Zone, Western rift, and their volcanological implications. Tectonophysics 209: 255–257.

Tables

Table 1 – Summary of the Nyamuragira eruptions analysed in this study.

Figure Captions

Figure 1 - (a) Shaded relief map of the Nyamuragira-Nyiragongo volcanic complex; (b) to (g) Location and extension of MODIS-derived thermal anomalies recorded during the analysed eruptions of Nyamuragira (see the text for explanation). (h) Long-term time-series of Volcanic Radiative Power (*VRP;* black stem) related to Nyamuragira eruptions between 2001 and 2012.

Figure 2 - Detailed *VRP* time-series (left axes on logarithmic scale) and cumulative *Volcanic Radiative Energy* (right axes, in red) for the analysed eruptions (from a to f). Symbols: *High-Radiating Regimes* (*HRR* - red squares), *Moderate-Radiating Regimes* (*MRR* - yellow triangles) and *Low-Radiating Regimes* (*LRR* - black diamonds). The so called "unsuitable" data are also shown with grey circles. The *Low Radiating Regime* is considered to represent a residual thermal anomaly associated to the lava flow cooling. The vertical lines indicate the timing of last detection that falls within *Moderate-Radiating Regimes* (hereby considered the end of each eruption).

Figure 3 – (a) Frequency histogram of *log[VRP]* recorded at Nyamuragira between 2001 and 2012 (with at least two main regimes of thermal radiation). (b) Log-normal probability plot for *VRP* data; (c) and (d) illustrate the frequency histogram and log-normal probability plot for VRP_{MAX} data (see the text for details on VRP_{MAX}). Three main statistical groups are recognised, being consistent with the occurrence of three radiating regimes (*Low*, *Moderate* and *High*)

Figure 4 –*Normalised Thermal Index* (*NTI*) maps related to the High (a), Moderate (b) and Low (c) Radiation Regimes recorded during the 2002 eruption of Nyamuragira. Note how the transition from *High-Radiating Regime (HRR)* to *Moderate-Radiating Regime (MRR)* is accompanied by the

focussing of the thermal anomaly around the vent area. This evolution is ascribed to the transition from a typical *high-rate effusive activity* (lava flows) to an *open vent activity* associated the final stage of each eruption. The *LRR* is likely associated with the cooling of the lava flow field. The maps are obtained by displaying the *NTI* (Wright et al. 2002) of each MODIS pixel (according to a normalised colour-scale) over a shaded relief map of the volcano (in transparency); Digital Elevation Model courtesy of CGIAR (srtm.csi.cgiar.org).

Figure 5 –*TADR* time-series for the 2001 eruption. Selected thermal images show the location and extension of thermal anomalies produced by lava flows (Time Averaged lava Discharge Rates for the northern and southern flows are shown by dotted and dashed lines, respectively). The grey bars are in correspondence of the selected scenes showed below.

Figure 6 – *TADR* time-series of the 2002 eruption with selected thermal images showing the location and extension of the thermal anomalies produced by lava flows. The grey bars are in correspondence of the selected scenes showed below. The black star indicates a field measurement (from Smithsonian Institution, 2002).

Figure 7 – *TADR* time-series of the 2004 eruption with selected thermal images showing the location and extension of the thermal anomalies produced by lava flows. The grey bars are in correspondence of the selected scenes showed below.

Figure 8 – *TADR* time-series of the 2010 eruption with selected thermal images that shows the location and extension of the thermal anomalies produced by lava flows. The grey bars are in correspondence of the selected scenes showed below.

Figure 9 – *TADR* time-series of the 2011-2012 eruption with selected thermal images showing the location and extension of the thermal anomalies produced by the related lava flows. The grey bars are in correspondence of the selected scenes showed below.

Figure 10 – (a) Relationships between MODIS-derived volumes and the final lava flow areas reported by Smet et al., (2010). Straight dashed lines indicate the volumes obtained for different flow thicknesses. The grey field envelops our best volume estimates for the 2001, 2002, 2004 and 2010; (b) Relationships between MODIS-derived volumes and the duration of the *Low-Radiating Regime* (*LRR*) ascribed to the cooling of the lava flow fields. The linear correlation supports the causal link between the erupted volume and the duration of the cooling process.

Supplementry material

Within the supplementary material we provided a full description of the method used to correct the *VRP* for MODIS band 21 saturation.

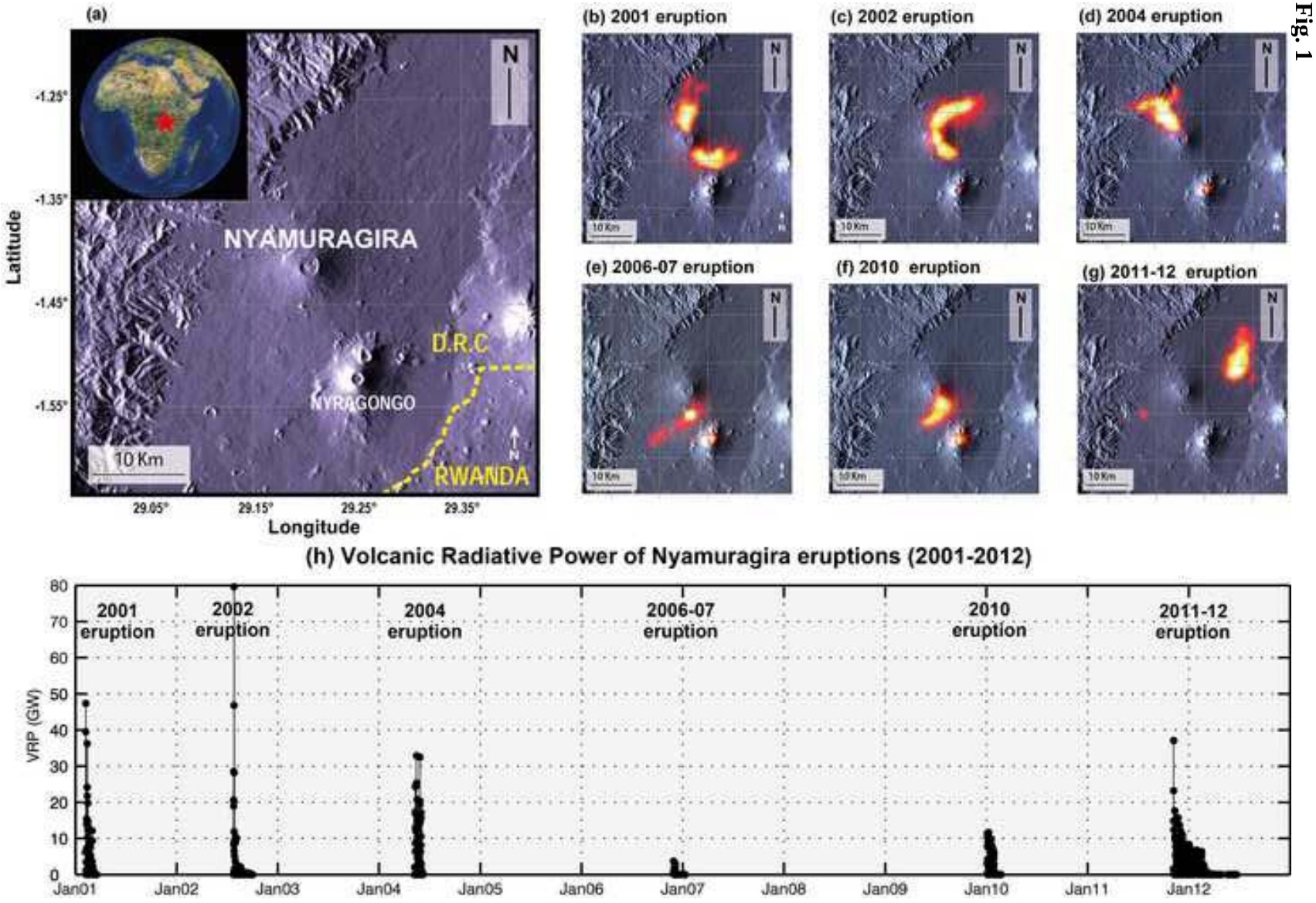
(a)
NYAMURAGIRA
NYRAGONGO
D.R.C
RWANDA
10 Km
N
-1.25°
-1.35°
-1.45°
-1.55°
Latitude
29.05°
29.15°
29.25°
29.35°
Longitude
(b) 2001 eruption
(c) 2002 eruption
(d) 2004 eruption
(e) 2006-07 eruption
(f) 2010 eruption
(g) 2011-12 eruption
(h) Volcanic Radiative Power of Nyamuragira eruptions (2001-2012)
2001 eruption
2002 eruption
2004 eruption
2006-07 eruption
2010 eruption
2011-12 eruption
VRP (GW)
0
10
20
30
40
50
60
70
80
Jan01
Jan02
Jan03
Jan04
Jan05
Jan06
Jan07
Jan08
Jan09
Jan10
Jan11
Jan12

Fig. 1

Fig. 2

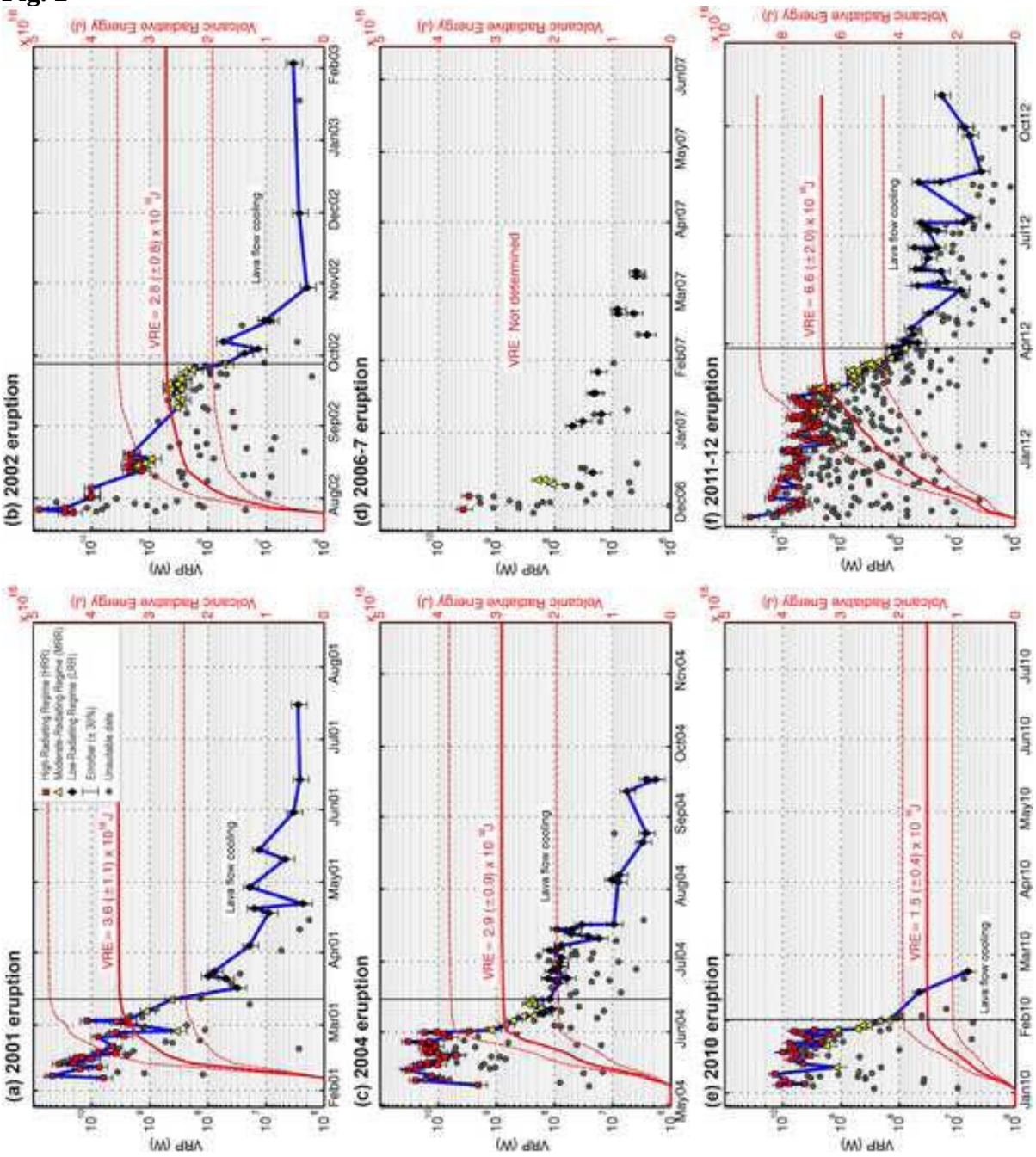
(a) 2001 eruption
(b) 2002 eruption
(c) 2004 eruption
(d) 2006-7 eruption
(e) 2010 eruption
(f) 2011-12 eruption
VRE = 3.6 (±1.1) x 10^15 J
VRE = 2.8 (±0.8) x 10^15 J
VRE = 2.9 (±0.9) x 10^15 J
VRE: Not determined
VRE = 1.5 (±0.4) x 10^15 J
VRE = 6.6 (±2.0) x 10^15 J
Lava flow cooling
VRP (W)
Volcanic Radiative Energy (J)

Fig. 3

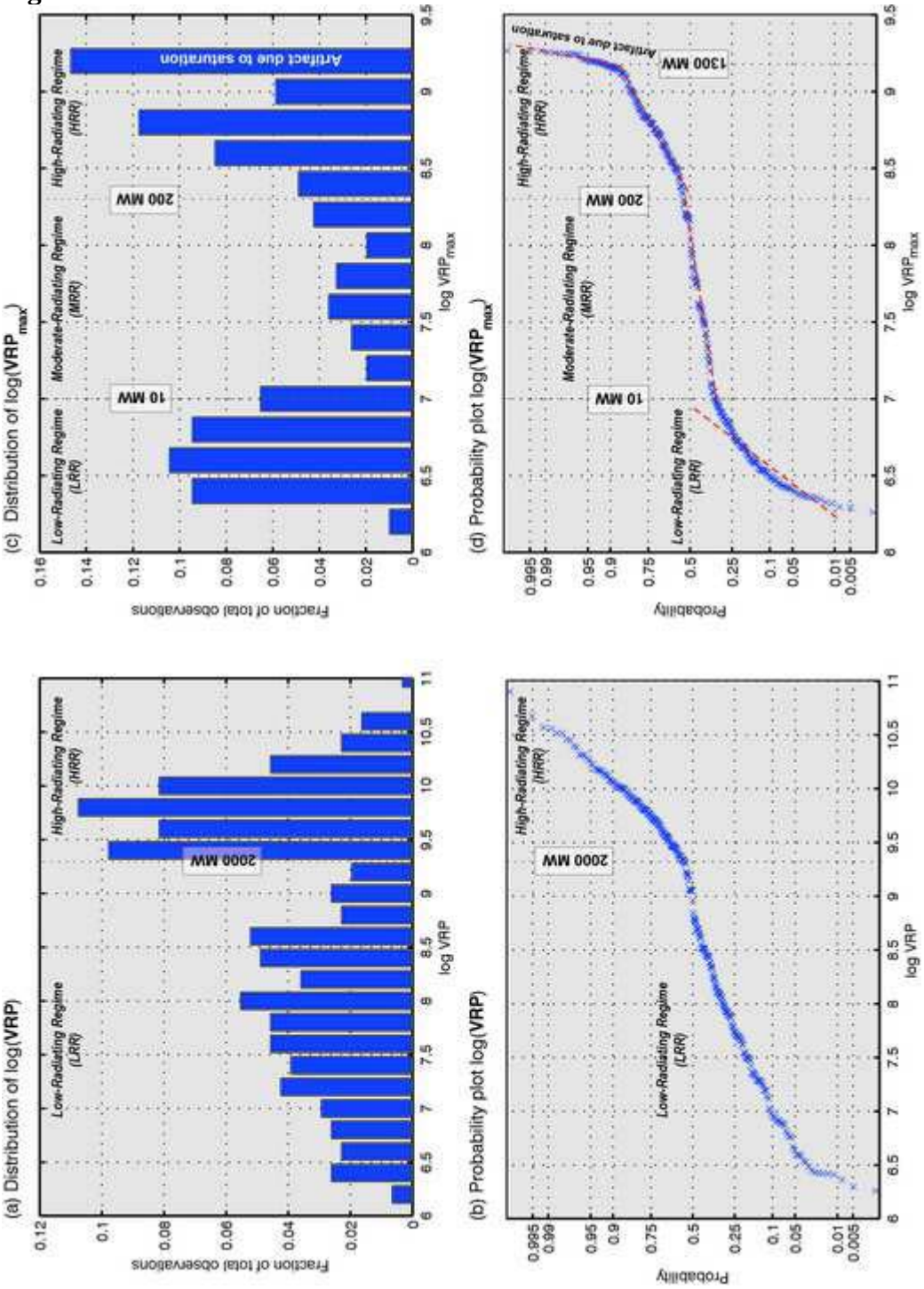
(a) Distribution of log(VRP)
(b) Probability plot log(VRP)
(c) Distribution of log(VRP$_{max}$)
(d) Probability plot log(VRP$_{max}$)
Low-Radiating Regime (LRR)
Moderate-Radiating Regime (MRR)
High-Radiating Regime (HRR)
10 MW
200 MW
1300 MW
2000 MW
Artifact due to saturation
Fraction of total observations
Probability
log VRP
log VRP$_{max}$

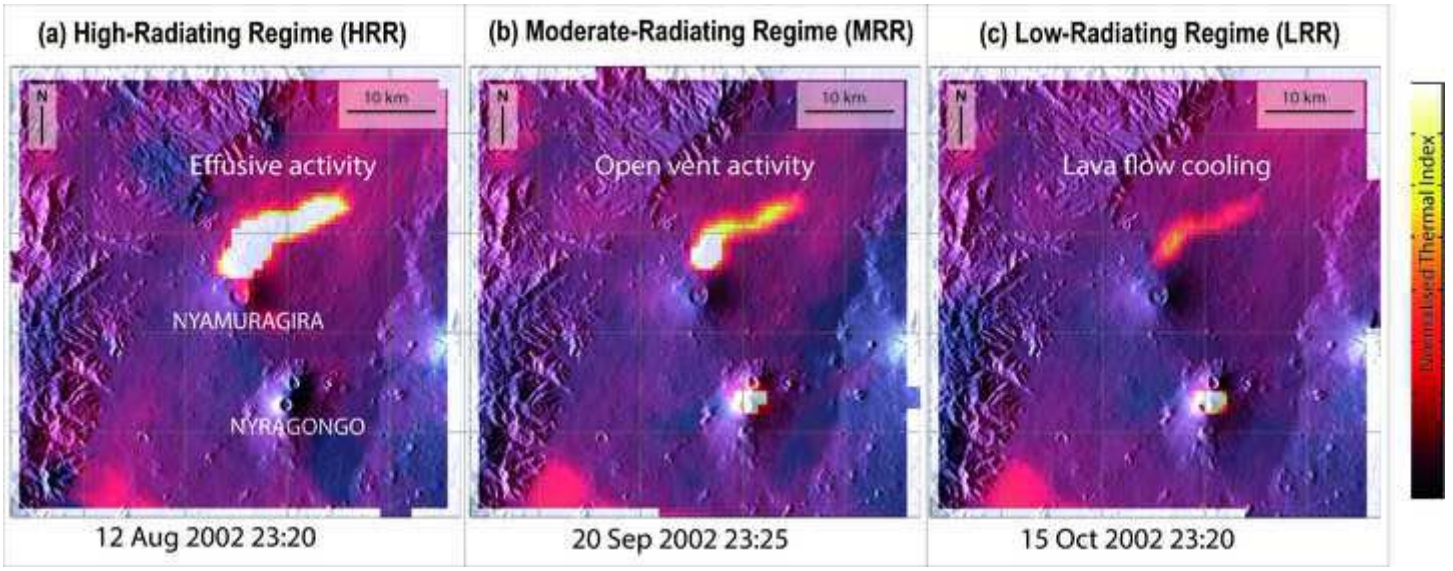
(a) High-Radiating Regime (HRR)
(b) Moderate-Radiating Regime (MRR)
(c) Low-Radiating Regime (LRR)
N
10 km
Effusive activity
NYAMURAGIRA
NYRAGONGO
Open vent activity
Lava flow cooling
Normalized Thermal Index
12 Aug 2002 23:20
20 Sep 2002 23:25
15 Oct 2002 23:20

Fig. 4

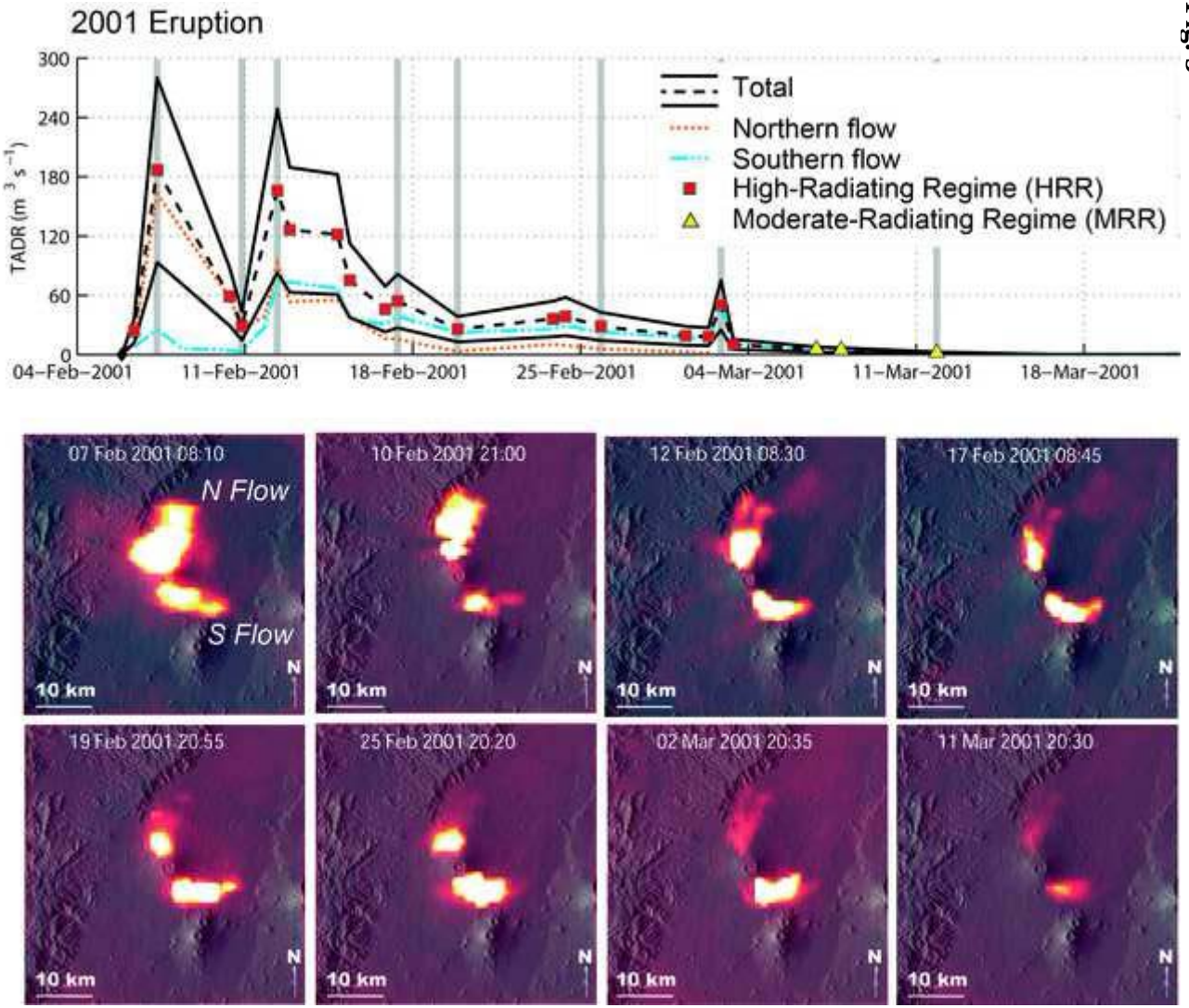
2001 Eruption
TADR (m 3 s −1)
300
240
180
120
60
0
04–Feb–2001
11–Feb–2001
18–Feb–2001
25–Feb–2001
04–Mar–2001
11–Mar–2001
18–Mar–2001
Total
Northern flow
Southern flow
High-Radiating Regime (HRR)
Moderate-Radiating Regime (MRR)
07 Feb 2001 08:10
N Flow
S Flow
10 Feb 2001 21:00
12 Feb 2001 08:30
17 Feb 2001 08:45
19 Feb 2001 20:55
25 Feb 2001 20:20
02 Mar 2001 20:35
11 Mar 2001 20:30
10 km
N

Fig. 5

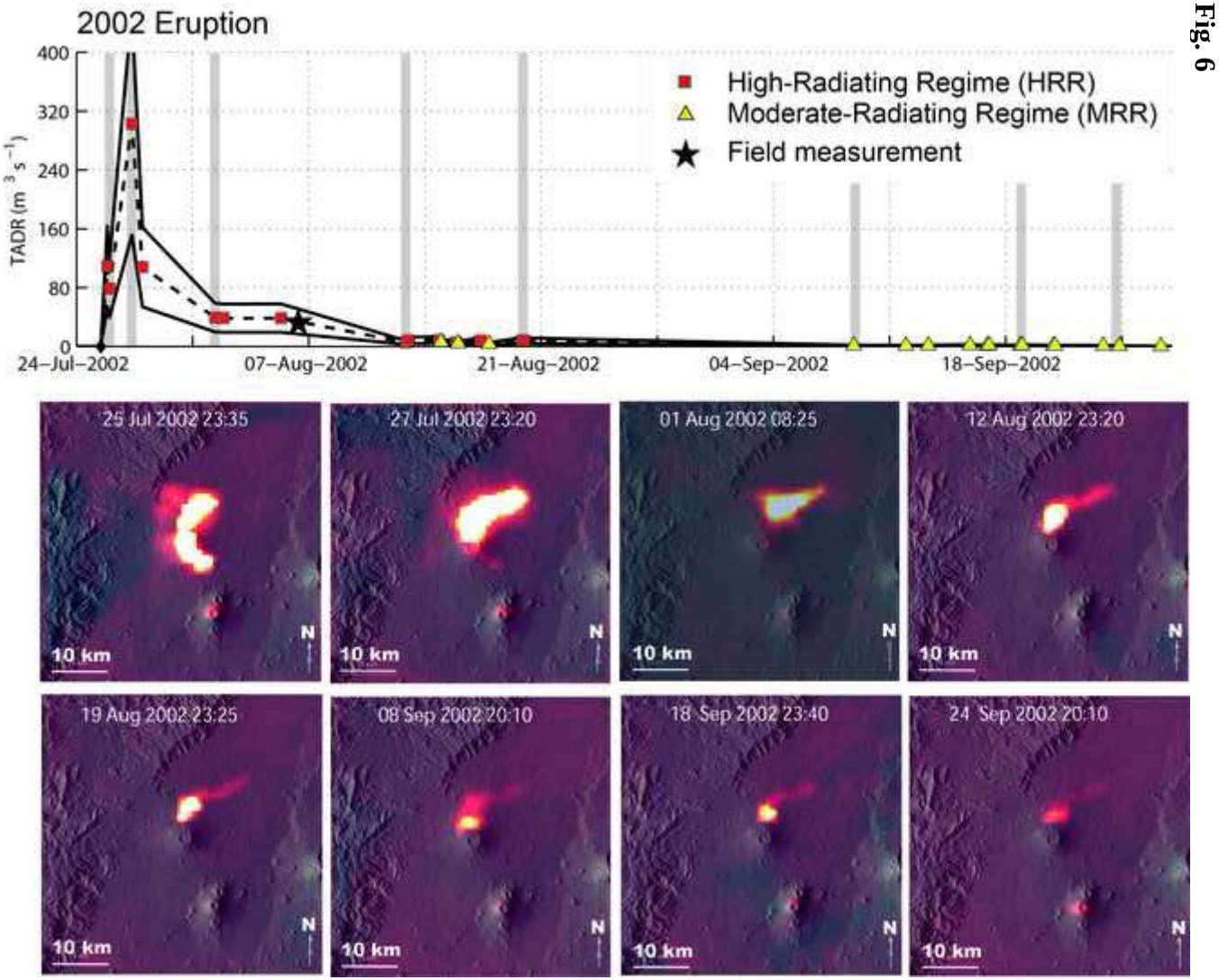
2002 Eruption
TADR (m 3 s −1)
400
320
240
160
80
0
24–Jul–2002
07–Aug–2002
21–Aug–2002
04–Sep–2002
18–Sep–2002
High-Radiating Regime (HRR)
Moderate-Radiating Regime (MRR)
Field measurement
25 Jul 2002 23:35
27 Jul 2002 23:20
01 Aug 2002 08:25
12 Aug 2002 23:20
19 Aug 2002 23:25
08 Sep 2002 20:10
18 Sep 2002 23:40
24 Sep 2002 20:10
10 km
N

Fig. 6

Fig. 7

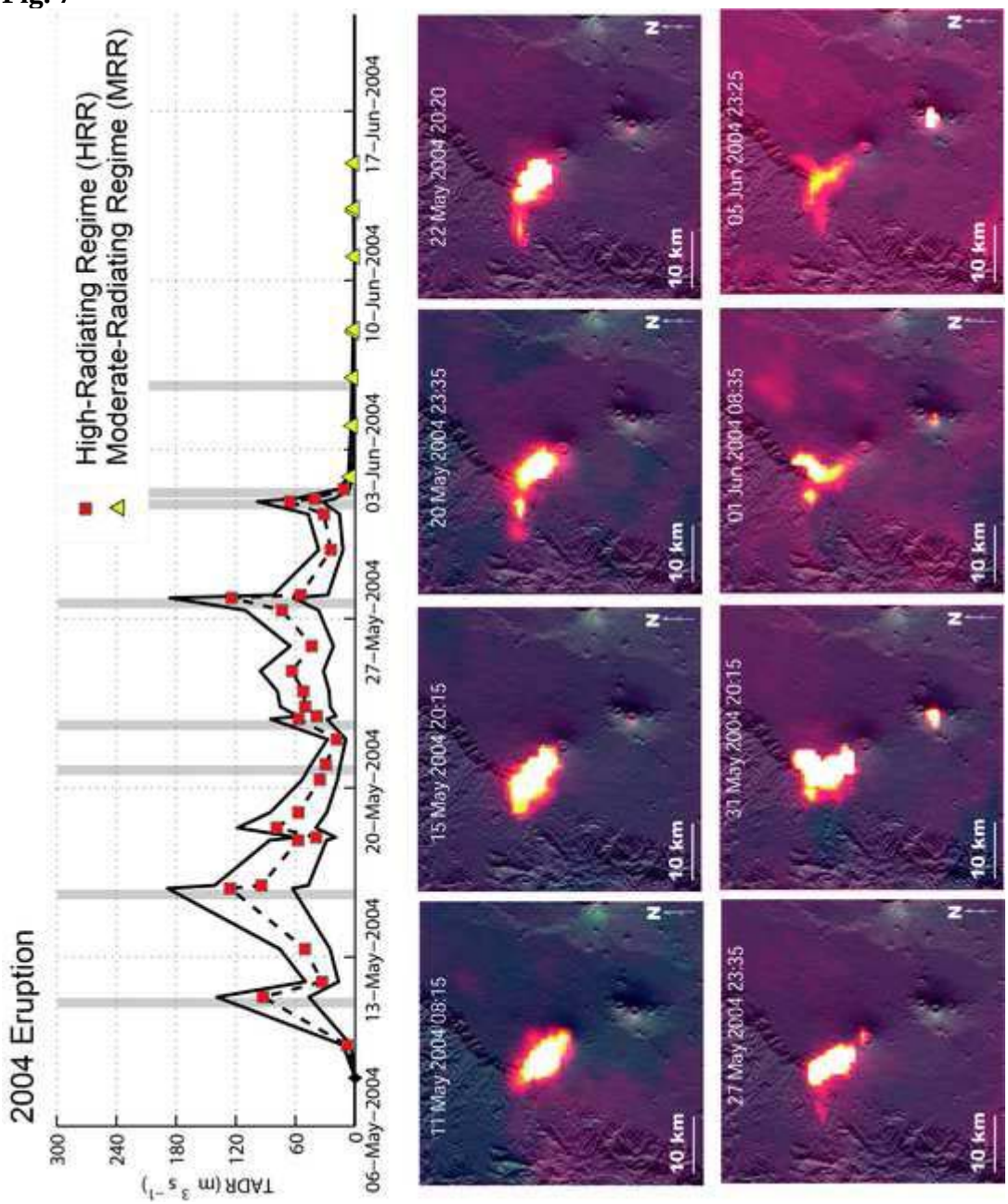
2004 Eruption
High-Radiating Regime (HRR)
Moderate-Radiating Regime (MRR)
TADR (m³ s⁻¹)
300
240
180
120
60
0
06–May–2004
13–May–2004
20–May–2004
27–May–2004
03–Jun–2004
10–Jun–2004
17–Jun–2004
11 May 2004 08:15
15 May 2004 20:15
20 May 2004 23:35
22 May 2004 20:20
27 May 2004 23:35
31 May 2004 20:15
01 Jun 2004 08:35
05 Jun 2004 23:25
N
10 km

Fig. 8

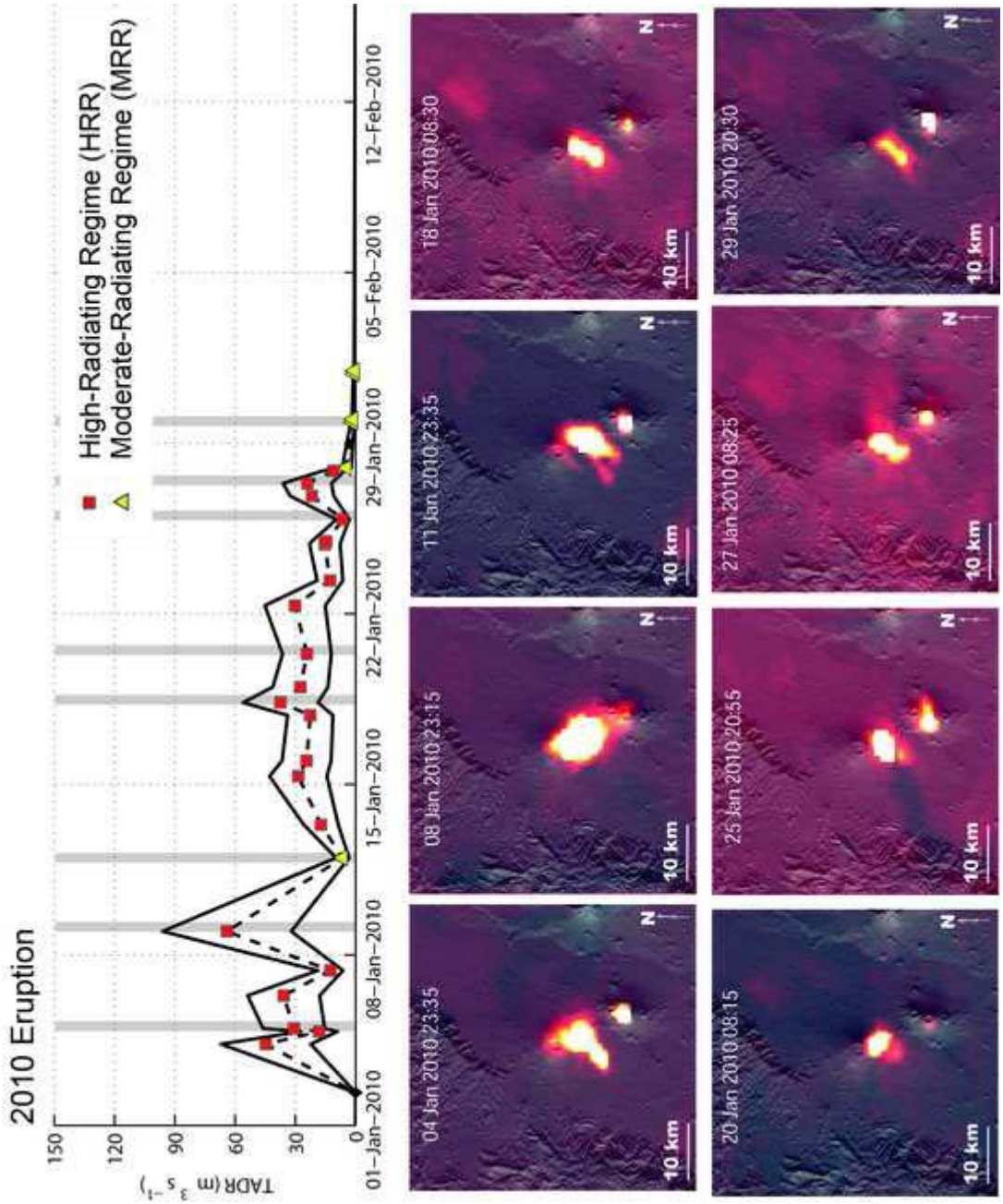
2010 Eruption
High-Radiating Regime (HRR)
Moderate-Radiating Regime (MRR)
TADR (m 3 s −1)
150
120
90
60
30
0
01–Jan–2010
08–Jan–2010
15–Jan–2010
22–Jan–2010
29–Jan–2010
05–Feb–2010
12–Feb–2010
04 Jan 2010 23:35
08 Jan 2010 23:15
11 Jan 2010 23:35
18 Jan 2010 08:30
20 Jan 2010 08:15
25 Jan 2010 20:55
27 Jan 2010 08:25
29 Jan 2010 20:30
N
10 km

Fig. 9

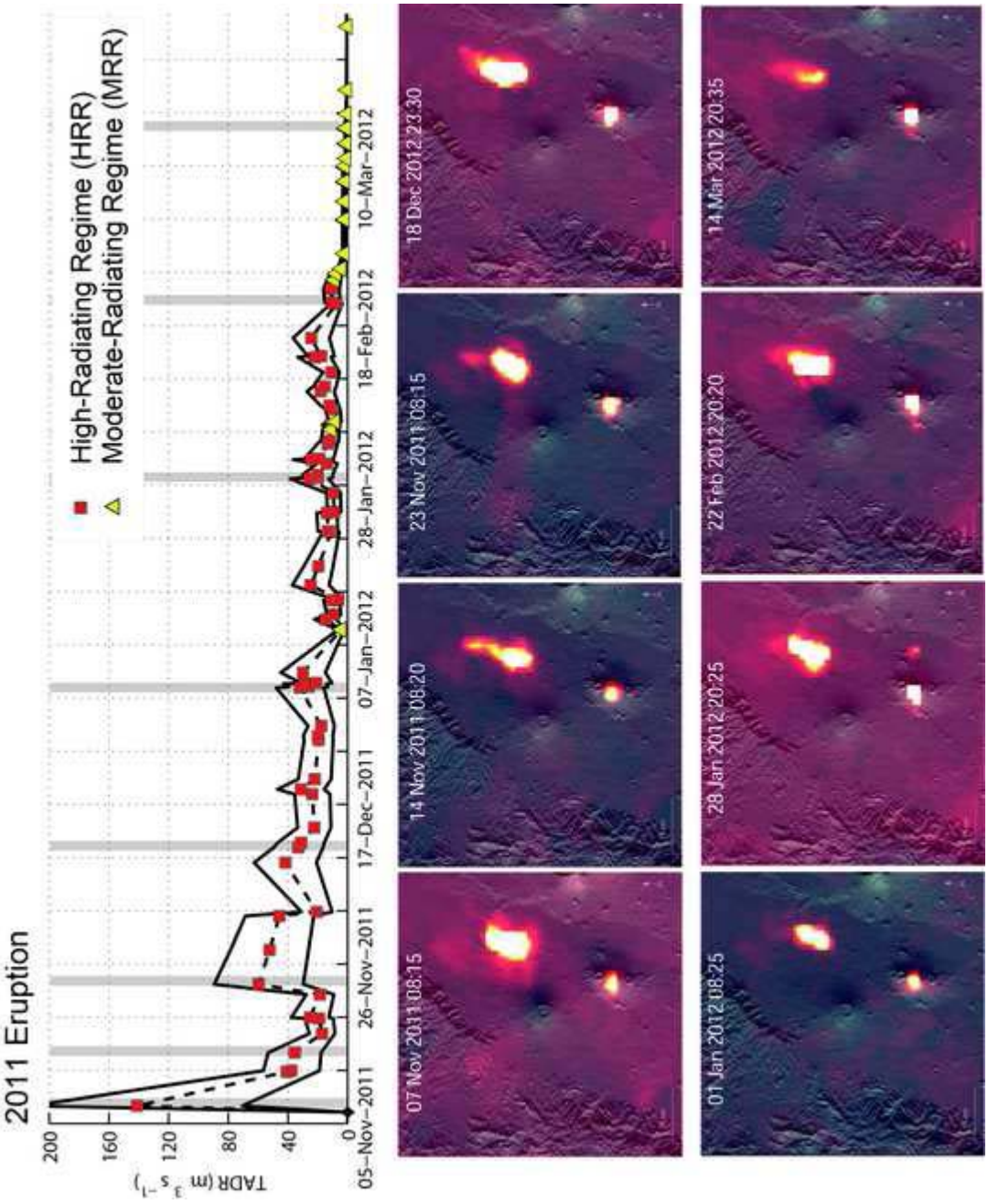
2011 Eruption
High-Radiating Regime (HRR)
Moderate-Radiating Regime (MRR)
TADR (m 3 s −1)
200
160
120
80
40
0
05–Nov–2011
26–Nov–2011
17–Dec–2011
07–Jan–2012
28–Jan–2012
18–Feb–2012
10–Mar–2012
07 Nov 2011 08:15
14 Nov 2011 08:20
23 Nov 2011 08:15
18 Dec 2012 23:30
01 Jan 2012 08:25
28 Jan 2012 20:25
22 Feb 2012 20:20
14 Mar 2012 20:35

Fig. 11

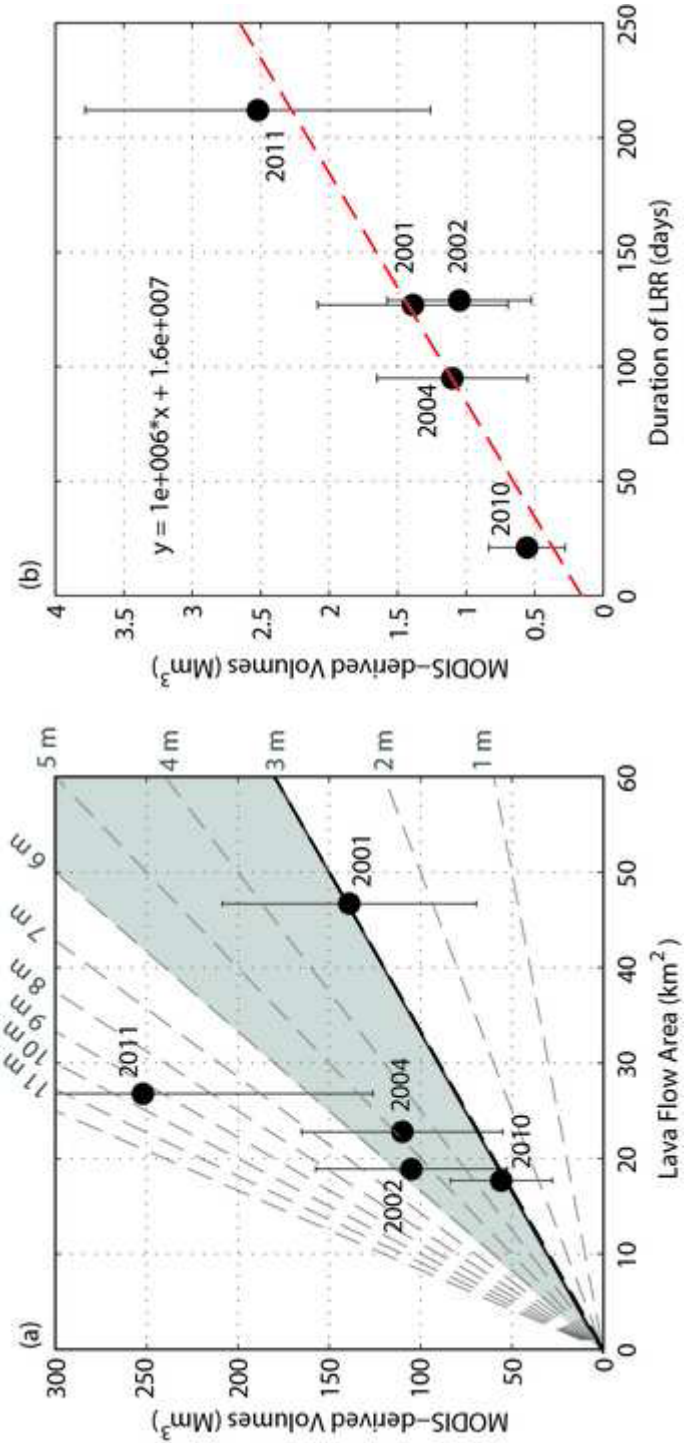
(a)
MODIS–derived Volumes (Mm³)
Lava Flow Area (km²)
1 m
2 m
3 m
4 m
5 m
6 m
7 m
8 m
9 m
10 m
11 m
2001
2004
2002
2010
2011
(b)
MODIS–derived Volumes (Mm³)
Duration of LRR (days)
y = 1e+006*x + 1.6e+007
2001
2002
2004
2010
2011

Table 1

Nyamuragira Eruption year	beginning[1]	*Analysed* end_{HRR}[2]	*period* end_{MRR}[2]	end_{LRR}[2]	*Duration HRR* days	*Duration MRR* days	*Duration HRR+MRR* days	*Duration LRR* days	*VRE* MODIS (+30%) J	Volume MODIS (+50%) m^3	Area flow mapping[3] m^2	H[5] (+50%) m
2001	05/02/2001	03/03/2001	11/03/2001	16/07/2001	26	8	34	127	3.65E+16	1.39E+08	4.67E+07	3.0
2002	25/07/2002	19/08/2002	27/09/2002	02/02/2003	26	38	64	129	2.77E+16	1.05E+08	1.89E+07	5.6
2004	07/05/2004	01/06/2004	14/06/2004	17/09/2004	24	13	38	95	2.90E+16	1.10E+08	2.28E+07	4.8
2006-7	27/11/2006	04/12/2006	11/12/2006	10/03/2007	8	7	15	89	N.d.	N.d.	1.47E+07	N.d.
2010	02/01/2010	27/01/2010	31/01/2010	21/02/2010	25	4	29	21	1.47E+16	5.58E+07	1.77E+07	3.2
2011-12	06/11/2011	24/02/2012	28/03/2012	26/10/2012	110	33	143	212	6.63E+16	2.52E+08	2.68E+07[4]	9.4

(1) from Smithsonian Institution (2001 to present)
(2) last detection in each thermal regime
(3) from Smet et al. 2010
(4) this work
(5) MODIS-derived olumes divided by flow area